

## Get Clarity On Generics

Cost-Effective CT & MRI Contrast Agents



FRESENIUS  
KABI

WATCH VIDEO

# AJNR

## Premature fat deposition in the salivary glands associated with Sjögren syndrome: MR and CT evidence.

M Izumi, K Eguchi, H Nakamura, S Nagataki and T Nakamura

This information is current as of August 27, 2025.

*AJNR Am J Neuroradiol* 1997, 18 (5) 951-958  
<http://www.ajnr.org/content/18/5/951>

# Premature Fat Deposition in the Salivary Glands Associated with Sjögren Syndrome: MR and CT Evidence

Masahiro Izumi, Katsumi Eguchi, Hideki Nakamura, Shigenobu Nagataki, and Takashi Nakamura

**PURPOSE:** To investigate abnormal fat deposition in the major salivary glands associated with Sjögren syndrome. **METHODS:** We analyzed the fat deposition in the parotid and submandibular glands of 33 patients with Sjögren syndrome by using short-inversion-time inversion recovery (STIR) and fat-saturation MR sequences and CT values. **RESULTS:** All three in vivo techniques substantially confirmed premature deposition of fat in the major salivary glands in association with Sjögren syndrome. Furthermore, this change was characteristic of Sjögren syndrome, and the severity of fat deposition correlated well with the impaired rates of salivary flow in these patients. **CONCLUSION:** Monitoring of fat deposition might be useful for diagnosing Sjögren syndrome and assessing its progress in patients whose clinical and serologic findings are suggestive of the disease.

**Index terms:** Eyes, diseases; Salivary glands, magnetic resonance; Magnetic resonance, fat suppression

*AJNR Am J Neuroradiol* 18:951-958, May 1997

Sjögren syndrome is an autoimmune disease characterized by lymphocytic infiltration in exocrine glands, such as the salivary and lacrimal glands, resulting in dry mouth and dry eyes (1). Characteristic features of gland parenchyma include lymphocyte infiltration, disappearance of acinus, and fibrosis (1). At present, our knowledge is limited as to the pathologic changes taking place in the major salivary glands of patients with this disorder. Recently, investigators have established magnetic resonance (MR) imaging characteristics of the parotid gland in patients with Sjögren syndrome (2), including high-intensity signal on T1-weighted MR images, which may indicate the presence of hemorrhage, proteinaceous content, or fat tissue.

One of the most exciting innovations in MR imaging over the past several years has been the development of a fat-suppression technique

(3), which has been used successfully in many fields of MR diagnosis (4-8). Two major methods of fat suppression are the short-inversion-time inversion recovery (STIR) and the fat-saturation sequences (3, 9). The STIR sequence suppresses signal from tissues that have short T1 values, similar to fat tissues; the fat-saturation technique, on the other hand, uses the chemical-shift phenomenon to suppress signal from fat tissues. Computed tomography (CT) is also a useful tool for determining the presence of fat tissue, since the CT value, which is based on tissue-specific X-ray absorption, can help differentiate fat tissue from other soft-tissue body components, such as water, muscle, and even gland parenchyma.

The purpose of this study was to assess the changes in the major salivary glands in patients with Sjögren syndrome by using the STIR and fat-saturation MR sequences and CT. We show that fat deposition develops early in the course of the disease and that the changes correspond to the severity of salivary flow dysfunction.

## Subjects and Methods

### Subjects

The MR study population included 20 women (34 to 72 years old; mean,  $52 \pm 11$  years) with definite Sjögren

---

Received August 26, 1996; accepted after revision December 2.

From the Department of Radiology, Nagasaki (Japan) University School of Dentistry (M.I., T.N.), and the First Department of Internal Medicine, Nagasaki University School of Medicine (K.E., H.N., S.N.).

Address reprint requests to Takashi Nakamura, DDS, PhD, Department of Radiology, Nagasaki University School of Dentistry, 1-7-1 Sakamoto, Nagasaki 852, Japan.

AJNR 18:951-958, May 1997 0195-6108/97/1805-0951

© American Society of Neuroradiology

syndrome and 13 women (29 to 69 years old; mean,  $48 \pm 14$  years) with probable Sjögren syndrome. Twenty-seven healthy women (25 to 68 years old; mean,  $55 \pm 17$  years) served as control subjects. The patients with definite disease included 18 with primary and two with secondary Sjögren syndrome (rheumatoid arthritis overlapped in two patients). The patients with probable disease included seven with primary and six with secondary Sjögren syndrome (rheumatoid arthritis overlapped in four patients, systemic lupus erythematosus overlapped in one, and CREST [calcinosis, Raynaud phenomenon, esophageal dysmotility, sclerodactyly, telangiectasia] syndrome overlapped in one). Patients with definite Sjögren syndrome met all the criteria raised by Fox et al (1). Patients with probable Sjögren syndrome lacked the criteria on labial gland biopsy but were positive for the other criteria. The CT study population included the 33 patients with Sjögren syndrome used in the MR study and 110 subjects (19 to 84 years old; mean,  $51 \pm 15$ ) reported to have no history of disease or treatment that could affect the salivary glands. These persons were used as control subjects for assessment of age-related changes in CT values. Informed consent was obtained from the patients who participated in the investigation.

#### MR Imaging and Grading of Sjögren Syndrome

MR imaging at 1.5 T was performed in the parotid and submandibular glands of patients with Sjögren syndrome and control subjects. A head coil was used for the parotid glands and a cervical coil for the submandibular glands. Axial T1-weighted (500/20/2 [repetition time/echo time/excitations]) and T2-weighted (2000/80) images were obtained by use of a conventional spin-echo sequence. For fat suppression, the STIR (1000/20; inversion time, 120) and fat-saturation (500/20/2) pulse sequences were used. Section thickness was 5 mm for all three sequences. Based on findings on the T1- and T2-weighted MR images, we classified the parotid gland into five grades as described previously (Table). The MR criteria for classification of the parotid gland in patients with Sjögren syndrome are clear-cut, and results of independent classification by two radiologists were similar in the present and previous (2) studies. According to the diagnostic criteria by Fox et al (1), the parotid glands in patients with definite Sjögren syndrome are classified as grades 2 to 4.

#### Grading system of parotid gland MR features

|                         | Grade |   |    |    |     |
|-------------------------|-------|---|----|----|-----|
|                         | 0     | 1 | 2  | 3  | 4   |
| High-intensity area on: |       |   |    |    |     |
| T1-weighted image       | —     | + | +  | ++ | +++ |
| T2-weighted image       | —     | — | +  | +  | —   |
| No. of patients         | 6     | 4 | 10 | 7  | 6   |

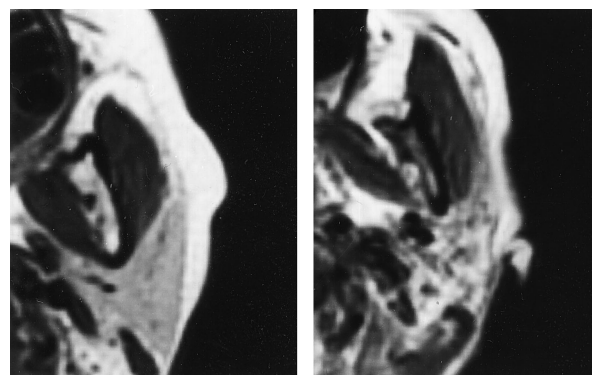


Fig 1. T1-weighted (500/20/2) MR features of parotid glands from healthy subject (A) and patient with Sjögren syndrome (B).

#### CT

CT of the parotid glands was performed in all 33 patients with Sjögren syndrome and in 110 control subjects. Axial 4-mm-thick sections were obtained and used to determine CT values in the parotid glands. The scan showing the maximum area of the parotid gland was used, and analyses were carried out on the cathode-ray tube display of the Somatom (Erlangen, Germany) DR-H scanner. A circular ( $0.84 \text{ cm}^2$ ) region of interest was manually placed within each gland. Such localization avoided overlapping of the main duct of the parotid gland and retromandibular vein.

#### Salivary Flow Rate Test

Salivary flow rates of each of the patients with Sjögren syndrome were quantified by the Saxon test and expressed as grams per 2 minutes, as described previously (10). A sterile gauze was placed in a sterile, screw-topped 50-mL plastic tube (Bluemax, Falcon Labware, Oxnard, Calif), and the dry gauze and tube were weighed. After any pre-existing oral fluid was removed, saliva was collected by having patients vigorously chew on the gauze for exactly 2 minutes. Salivary flow rate was determined by subtracting the original weight from the weight obtained after chewing.

#### Data Analysis

Differences in the salivary flow rates and in the CT values among MR grades were compared by Student's *t* test. Calculations were performed by Statview II software (Abacus Concepts, Berkeley, Calif).

#### Results

Multiple areas of high signal intensity appeared on T1-weighted images of the parotid glands affected by Sjögren syndrome in the early stages of the disease (Fig 1). When the

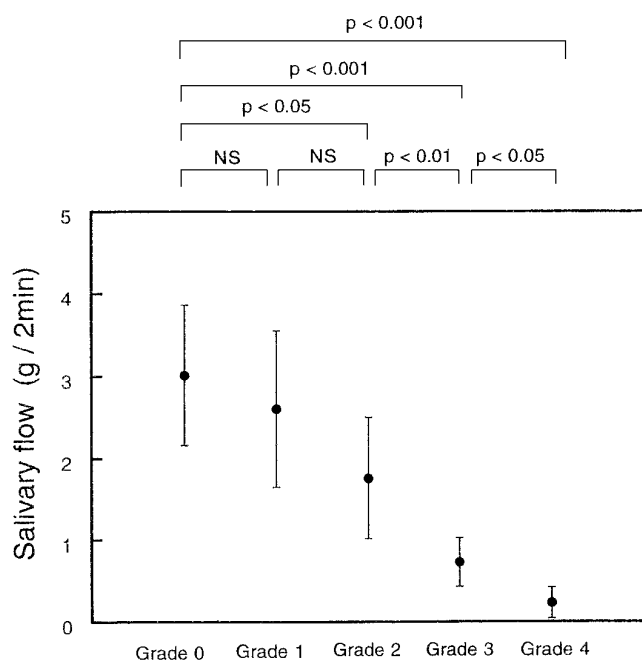


Fig 2. Salivary flow rates as determined by Saxon test in each grade of parotid gland in patients with Sjögren syndrome. Data represent means ( $\pm$ SD) of patients examined. NS means not significant.

parotid glands were tentatively classified into five grades on the basis of the appearance of high-intensity areas on T1- and T2-weighted images (Table), the grades correlated well with the severity of impaired salivary flow rates (Fig 2). Among patients who had received or who were being treated with steroid therapy, four had grade 0 glands, none had grade 1 glands, four had grade 2 glands, four had grade 3 glands, and one had grade 4 glands. However, we could not obtain evidence suggestive of the influence of steroids on the degree of fat deposition.

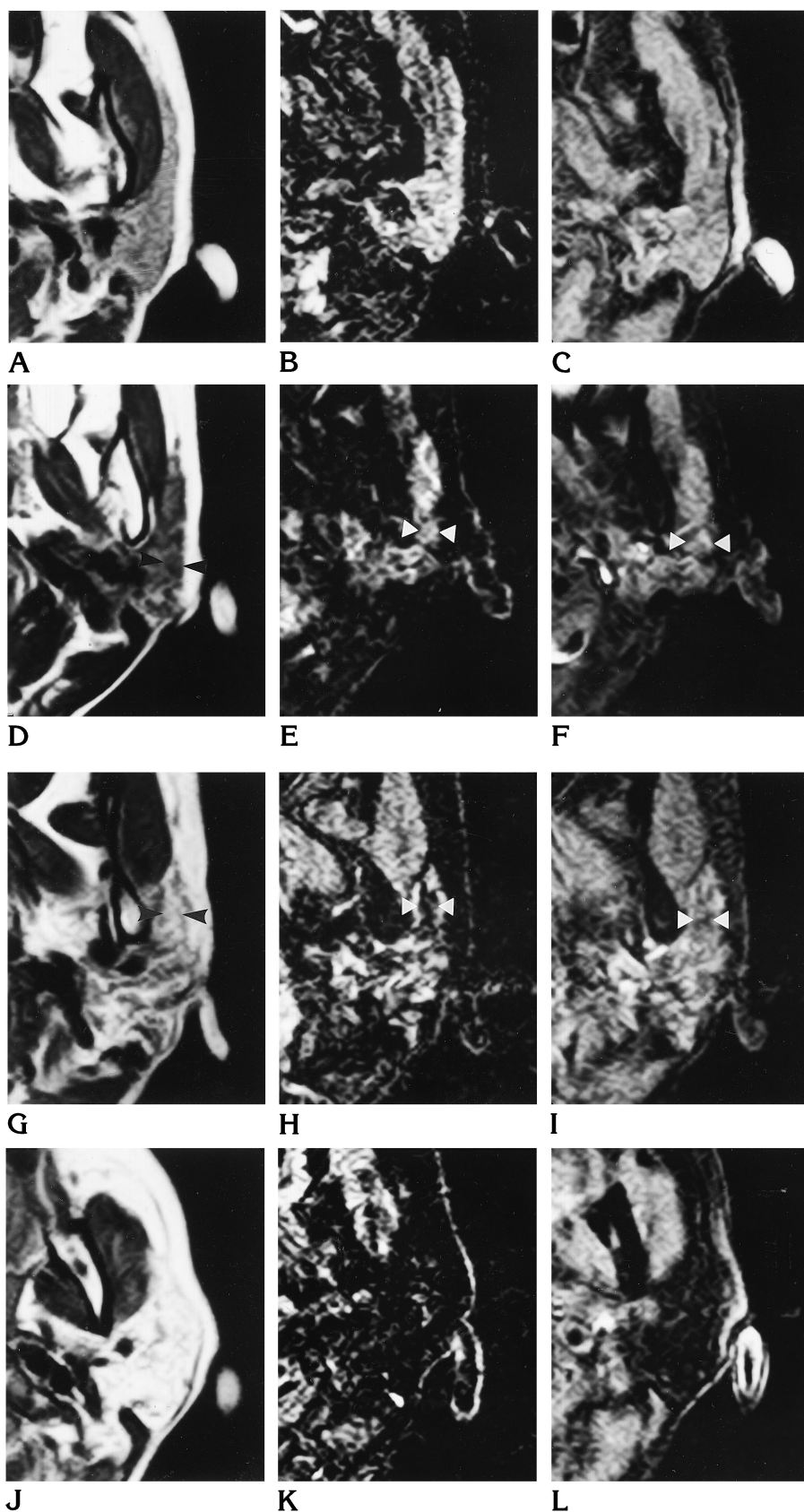
Given a close relationship between areas of high signal intensity and involvement of the parotid gland by Sjögren syndrome, we attempted to examine the cause of these high-intensity areas. The appearance of high-intensity areas on T1-weighted MR images of the parotid gland implied the presence of fat tissues. To test this, we used two unrelated *in vivo* MR methods: the STIR and fat-saturation sequences. Both methods showed decreased signal in areas that correlated with high-intensity signal on the T1-weighted images of the parotid glands affected by Sjögren syndrome. In patients with grade 1 glands, T1-weighted images showed multiple spots of high signal intensity (Fig 3A). The STIR sequence converted the parotid gland to a high

intensity-rich organ with multiple spots of low or no signal intensity, which corresponded to the high-intensity spots on T1-weighted images (Fig 3B). With advances in grade, the T1 high-intensity signal occupied more areas in the glands, appearing as streaks in grade 2 (Fig 3D), weblike structures in grade 3 (Fig 3G), and homogeneous high-intensity areas in grade 4 (Fig 3J). The STIR sequence readily suppressed these high-intensity signals (Fig 3E, H, and K). Since the STIR technique may be considered nonspecific (9), we next used a different fat-suppression technique, fat saturation. The fat-saturation sequence also successfully suppressed the high-intensity areas on T1-weighted images (Fig 3C, F, I, and L). These results suggest that the high-intensity areas on T1-weighted images of the parotid glands in patients with Sjögren syndrome are due to increasing fat deposition in the glands.

To substantiate this notion, we examined the parotid glands of Sjögren syndrome patients by CT, and evaluated tissue-specific X-ray absorption values (CT values). The CT scans showed increasing areas of low CT values in parallel with the advancement in the grade of the parotid gland as determined by MR criteria (Fig 4). The glands classified as grade 4 were almost completely replaced by fat tissue density (Fig 4C). When each CT value was expressed as a mean within a region of interest placed in each of the parotid glands, the normal parotid glands showed mean CT values of  $-14 \pm 14$  (Fig 5). Compared with the age- and sex-matched control subjects, mean CT values did not decrease significantly in the parotid glands of grades 0, 1, and 2. However, the parotid glands of grades 3 and 4 showed significantly lower mean CT values than did normal glands. On the other hand, mean CT values of the subcutaneous fat tissues in the buccal regions showed fairly constant mean CT values throughout the grades (Fig 5).

Because senile changes in the parotid gland were reportedly associated with fat degeneration, we assessed age-related changes in the fat tissue deposition in healthy subjects. Indeed, CT values of the parotid glands showed an age-related decrease (CT value =  $23.5 - 0.58$  years;  $r = -.45$ ;  $P < .0001$ ), with the mean CT value at age 50 being  $-4$  (Fig 6). However, this mean CT value was much higher than those in Sjögren syndrome patients with parotid glands of grades 3 and 4 (Fig 5). Taken together, these results suggest that premature fat deposition

Fig 3. Effects of fat-suppression sequences (STIR: 100/20/2, inversion time of 120; fat-saturation: 500/20/2) on the areas of high signal intensity on T1-weighted MR images (500/20/2) of parotid glands in Sjögren syndrome patients. A–C, grade 1; D–F, grade 2; G–I, grade 3; J–L, grade 4. In grade 2, area of lower intensity signal (*black arrowheads*) on T1-weighted image (D) becomes relatively bright (*white arrowheads*) on STIR (E) and fat-saturation (F) images. In grade 3, area of high signal intensity (*black arrowheads*) on T1-weighted image (G) is suppressed and becomes relatively dark on STIR (H) and fat-saturation (I) images.



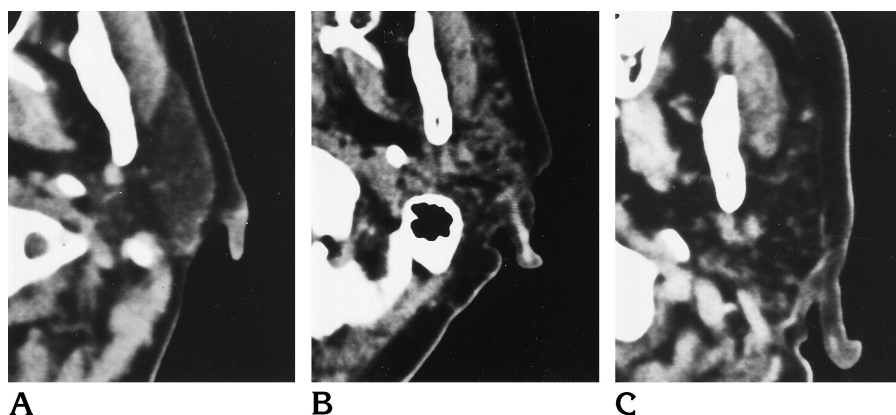


Fig 4. CT appearance of parotid glands in healthy subject (A) and in patients with Sjögren syndrome and grade 3 (B) and grade 4 (C) parotid glands.

occurred in the major salivary glands of Sjögren syndrome patients. Furthermore, the extensive fat deposition occurred in the submandibular glands as well as in the parotid glands, as assessed by MR imaging and CT (Fig 7).

Finally, the follow-up MR examinations of Sjögren syndrome patients suggested that fat deposition in the parotid glands progresses with advancement in the severity of disease. In one patient, grade 3 was classified about 2 years after the initial MR examination showed features of the parotid gland that were characteristic of grade 1 (Fig 8A and B). At the initial examination, this patient had negative results of lip biopsy and sialography, but she was positive for these examinations at the second MR study performed 2 years later. Another patient was found to have progressed from grade 2 to grade 3 during the 2-year follow-up period (Fig 8C and D).

## Discussion

Our study shows that fat deposition is definitely associated with the major salivary glands in patients with Sjögren syndrome as assessed by MR imaging and CT, and that its extent correlates with the severity of impaired salivary flow. Furthermore, the fat deposition occurred prematurely in the parotid glands of these patients. We used the STIR and fat-saturation sequences to show T1-weighted high intensity signal within some of the parotid glands in Sjögren syndrome patients and then to show that fat-suppressed sequences took away the areas of high T1-weighted signal. On the other hand, the areas of relatively lower intensity in the glands on the T1-weighted images became relatively bright on the STIR images. Therefore,

we concluded that the regions of high signal intensity within the parotid gland corresponded to fat and that areas of lower signal corresponded to fluid-filled spaces or fibrous tissues. Further, when fat completely replaced the gland, the entire area was dark on the fat-suppressed images.

At question is whether fat deposition in the major salivary glands is a change characteristic of Sjögren syndrome or a nonspecific consequence of the major salivary gland destruction caused by lymphocyte infiltration and the ensuing fibrosis. The observation that fat deposition developed with increasing age in normal major salivary glands, but to a much lesser extent compared with those of Sjögren syndrome patients, may support the latter notion. On the other hand, the diffusely scattered fat deposition as seen on MR images of the parotid glands in Sjögren syndrome patients was never observed in the inflammatory parotid glands as depicted on MR images (2). However, we encountered one case of inflammation, which showed fat deposition in the parotid gland. In that case, the fat appeared as localized and nodulelike areas of high intensity in the affected gland on the T1-weighted images, which was different from the features of the salivary gland affected by Sjögren syndrome. Garrett (11) described the difference in fat deposition between the senile and inflammatory changes of the salivary glands. In the normal glands of senile subjects, fat deposition occurred in the secretory cells and duct cells, whereas fat accumulated in the histiocytes in close vicinity of abscesses in the salivary glands with severe inflammation. He also examined a patient with Sjögren syndrome and showed that the alveolar tissue had been destroyed and replaced extensively by fat (11).

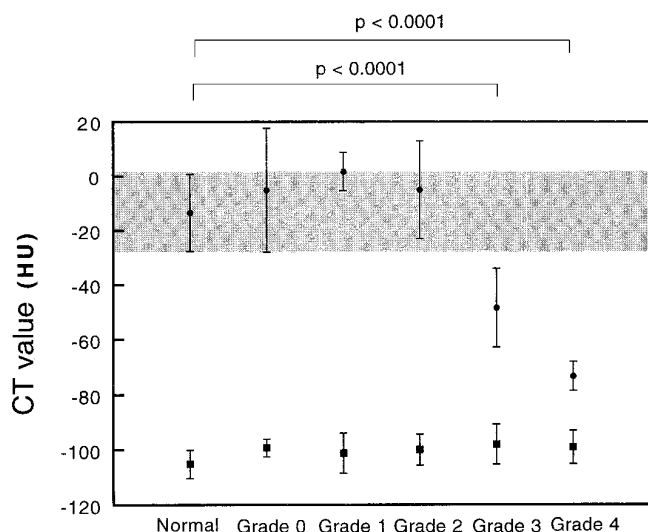


Fig 5. CT values of parotid glands in healthy subjects and in patients with Sjögren syndrome (grade 0–4 parotid glands). Circles indicate CT values of parotid glands; squares indicate CT values of subcutaneous fat; hatched area represents 1 SD of CT values of normal parotid glands.

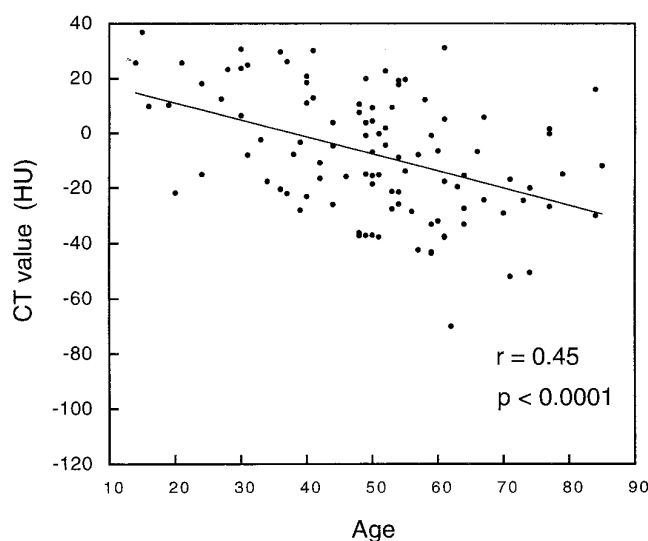


Fig 6. Age-related changes of parotid gland CT values in healthy subjects.

In addition, Block et al (12) examined the salivary glands from cadavers and showed that extensive fat tissue infiltrations occurred in the salivary glands of Sjögren syndrome patients, where minimal to moderate lymphocyte infiltrations were present. We also observed at autopsy an extensive replacement by fat of the submandibular glands in a patient with Sjögren syndrome. Taken together, these results suggest that, although fat deposition may occur in the repair process of damaged gland parenchyma, diffusely scattered and premature fat deposition

is characteristic of salivary glands affected by Sjögren syndrome.

At present, we do not know the exact mechanism of fat deposition in the salivary glands of Sjögren syndrome patients. The most straightforward scenario may be that parenchymal destruction caused by lymphocyte infiltration is followed by fibrosis. The proliferating fibroblasts are in turn induced to differentiate to adipocytes by cytokines and other differentiation mediators released by the surrounding lymphocytes or other cell types. Supporting this notion are several reports implying that immunologic factors play a role in fat synthesis (13, 14). Furthermore, peroxisome proliferator-activated receptor  $\gamma$  (PPAR- $\gamma$ ), which is one of the potent receptors regulating adipogenesis, is present in immune systems (15, 16). These results further suggest a close relationship between fat deposition and autoimmune diseases.

The clinical importance of the present findings may be twofold: first, fat deposition occurred even in the early stages of the disease, and thus could serve as a criterion for early diagnosis of Sjögren syndrome. This may be supported by our observation of a strong correlation between our MR grading system and sialographic or lip biopsy results (2). Furthermore, fat deposition in the salivary glands affected by Sjögren syndrome was found to progress in conjunction with advancement of the disease (Fig 8). Second, and more important, the extent of fat deposition paralleled the severity of salivary flow dysfunction in Sjögren syndrome patients (Fig 2). The classical criteria by lip biopsy do not disclose the extent of salivary gland tissue destruction in these patients, but simply show lymphocyte infiltration. These lip biopsy findings are not absolutely definitive for Sjögren syndrome, as they also occur in senile atrophy of the salivary glands (1). Fat deposition develops at the expense of the parenchyma of the salivary gland. This means that once the parenchyma is replaced by fat tissues, it will be lost forever.

One of the major limitations of the present study may be a lack of histopathologic confirmation in the salivary glands affected by Sjögren syndrome. Postmortem examinations have reportedly been performed in the salivary glands from Sjögren syndrome patients (11, 12); however, biopsy of the major salivary glands is thought to be very dangerous because of high risk of fistula formation after surgery and

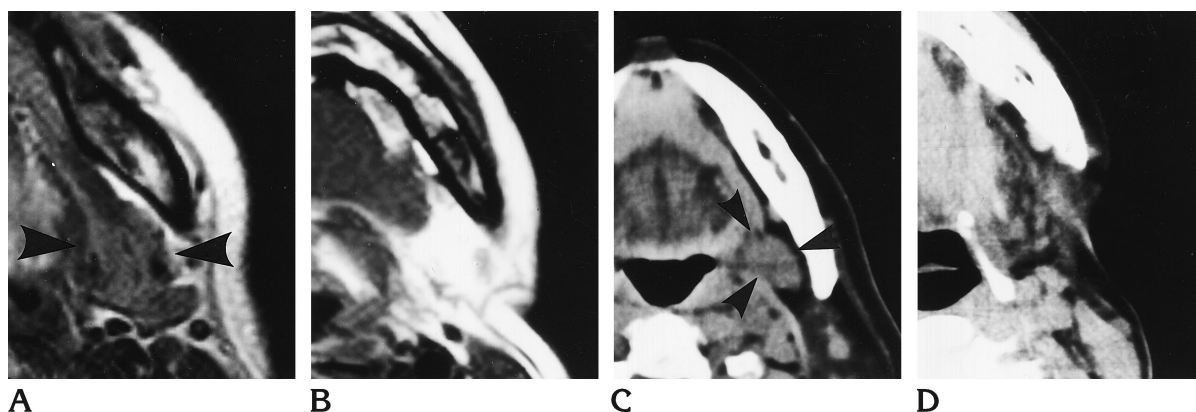


Fig 7. T1-weighted MR (500/20/2) (A and B) and CT (C and D) features of submandibular glands in healthy subject (A and C) and in patient with Sjögren syndrome (B and D). Arrowheads indicate submandibular glands in healthy subject. In patient with Sjögren syndrome, the gland is replaced by fat tissue and is not depicted on CT or MR images.

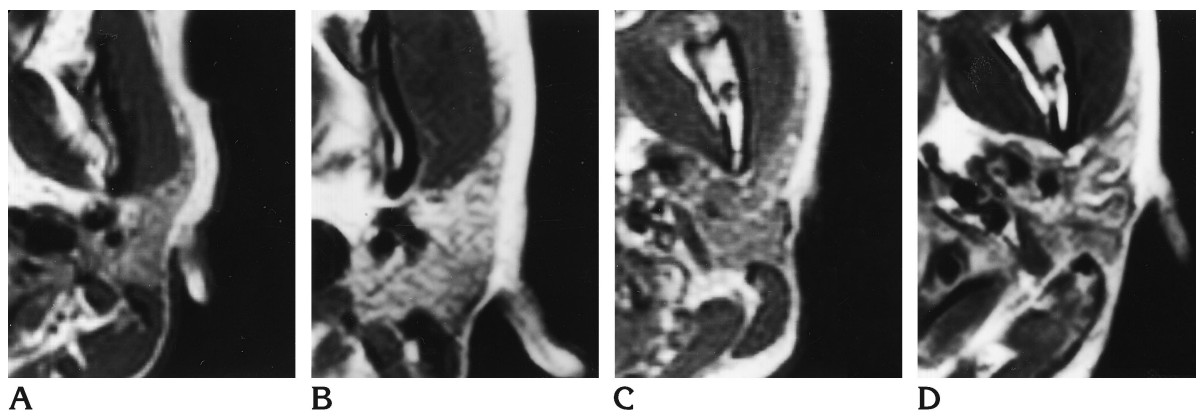


Fig 8. Two patients with Sjögren syndrome were found to have progressive fat deposition in the parotid glands during 2-year follow-up period. One patient had advanced from grade 1 (A) to grade 3 (B), and was determined to have definite Sjögren syndrome during this period. The other patient had advanced from grade 2 (C) to grade 3 (D).

of accidental damage to the overlying facial nerve. Therefore, we could not confirm fat deposition in the salivary glands in the patients in our study. Nonetheless, the present work may provide substantial evidence supporting the notion that fat deposition occurs prematurely in the major salivary glands in patients with Sjögren syndrome.

## References

1. Fox RI, Robinson CA, Curd JG, Kozin F, Howell FV. Sjögren's syndrome: proposed criteria for classification. *Arthritis Rheum* 1986;29:577-585
2. Izumi M, Eguchi K, Ohki M, et al. MR imaging of the parotid gland in Sjögren's syndrome: a proposal for new diagnostic criteria. *AJR Am J Roentgenol* 1996;166:1483-1487
3. Mirowitz SA. Fast scanning and fat-suppression MR imaging of musculoskeletal disorders. *AJR Am J Roentgenol* 1993;161:1147-1157
4. Mirowitz SA, Apicella P, Reinus WR, Hammerman AM. MR imaging of bone marrow lesions: relative conspicuousness on T1-weighted, fat-suppressed T2-weighted, and STIR images. *AJR Am J Roentgenol* 1994;162:215-221
5. Peterfy CG, van Dijke CF, Janzen DL, et al. Quantification of articular cartilage in the knee with pulsed saturation transfer subtraction and fat-suppressed MR imaging: optimization and validation. *Radiology* 1994;192:485-491
6. Gabata T, Matsui O, Kadoya M, et al. Small pancreatic adenocarcinomas: efficacy of MR imaging with fat suppression and gadolinium enhancement. *Radiology* 1994;193:683-688
7. Atlas SW, Grossman RI, Hackney DB, Goldberg HI, Bilaniuk LT, Zimmerman RA. STIR MR imaging of the orbit. *AJR Am J Roentgenol* 1988;151:1025-1030
8. Lamminen AE, Anttila V-JA, Bondestam S, Ruutu T, Ruutu PJ. Infectious liver foci in leukemia: comparison of short-inversion-time inversion-recovery, T1-weighted spin-echo and dynamic gadolinium-enhanced MR imaging. *Radiology* 1994;191:539-543
9. Krinsky G, Rofsky NM, Weinreb JC. Nonspecificity of short inversion time inversion recovery (STIR) as a technique of fat suppression: pitfalls in image interpretation. *AJR Am J Roentgenol* 1996;166:523-526



10. Kohler PF, Winter ME. A quantitative test for xerostomia; the Saxon test, an oral equivalent of the Schiermer test. *Arthritis Rheum* 1985;28:1128-1132
11. Garrett JR. Some observations on human submandibular salivary glands. *Proc Royal Soc Med* 1962;55:488-491
12. Block KJ, Buchanan WW, Wohl MJ, Bunim JJ. Sjögren's syndrome: a clinical, pathological, and serological study of sixty-two cases. *Medicine* 1965;44:187-231
13. Vernet C, Boretto J, Mattei MG, et al. Evolutionary study of multigenic families mapping close to the human MHC class I region. *J Mol Evol* 1993;37:600-612
14. Pham-Dinh D, Mattei MG, Nussbaum JL, et al. Myelin/oligodendrocyte glycoprotein in a member of a subset of the immunoglobulin superfamily encoded within the major histocompatibility complex. *Proc Natl Acad Sci U S A* 1993;90:7990-7994
15. Braissant O, Foufelle F, Scotto C, Dauça M, Wahli W. Differential expression of peroxisome proliferator-activated receptors (PPARs): tissue distribution of PPAR- $\alpha$ , - $\beta$ , and  $\gamma$  in the adult rats. *Endocrinology* 1996;137:354-366
16. Brun RP, Tontonoz P, Forman BM, et al. Differential activation of adipogenesis by multiple PPAR isoforms. *Genes Dev* 1996;10:974-984